Vortex structures formed by the interference of sliced condensates

R. Carretero-González,[1] N. Whitaker,[2] P. G. Kevrekidis,[2] and D. J. Frantzeskakis[3]

[1]*Nonlinear Dynamical Systems Group,* [*] *Department of Mathematics and Statistics, and Computational Science Research Center,*
San Diego State University, San Diego, California 92182-7720, USA
[2]*Department of Mathematics and Statistics, University of Massachusetts, Amherst, Massachusetts 01003-4515, USA*
[3]*Department of Physics, University of Athens, Panepistimiopolis, Zografos, Athens 15784, Greece*

We study the formation of vortices, vortex necklaces, and vortex ring structures as a result of the interference of higher-dimensional Bose-Einstein condensates (BECs). This study is motivated by earlier theoretical results pertaining to the formation of dark solitons by interfering quasi-one-dimensional BECs, as well as recent experiments demonstrating the formation of vortices by interfering higher-dimensional BECs. Here, we demonstrate the genericness of the relevant scenario, but also highlight a number of additional possibilities emerging in higher-dimensional settings. A relevant example is, e.g., the formation of a "cage" of vortex rings surrounding the three-dimensional bulk of the condensed atoms. The effects of the relative phases of the different BEC fragments and the role of damping due to coupling with the thermal cloud are also discussed. Our predictions should be immediately tractable in currently existing experimental BEC setups.

PACS number(s): 03.75.Lm, 03.75.Kk

I. INTRODUCTION

Shortly after the realization of atomic Bose-Einstein condensates (BECs) a remarkable experiment was reported [1], establishing BECs as coherent matter waves. This experiment demonstrated (apart from self-interference) the interference between two BECs confined in a trap, which was divided into two separate parts by means of a repulsive hump-shaped potential induced by a laser beam (usually called the "light sheet"). The BECs were left to expand and overlap, forming interference fringes, similar to the ones known in optics. Analysis of this phenomenon [2] allowed for a quantitative understanding of some of its key features (such as the fringe separation) based on the mean-field theory [3], and in particular the time-dependent Gross-Pitaevskii (GP) equation; the latter, can be expressed in the following dimensionless form (see, e.g., [4]):

$$i\frac{\partial u}{\partial t} = -\frac{1}{2}\nabla^2 u + V(\mathbf{r})u + |u|^2 u, \qquad (1)$$

where $u(\mathbf{r},t)$ is the condensate wave function [and $|u(\mathbf{r},t)|^2$ is the atom density], while $V(\mathbf{r})$ is the trapping potential. In fact, this potential is also time dependent since it has initially a double-well form (and the condensate is allowed to relax to its ground state) and subsequently, at $t=0$, the hump separating the two wells is lifted; in this way, the two fractions of the BEC are allowed to interfere and produce the beautiful experimental pictures observed (see, e.g., the observed pattern in Fig. 2 of Ref. [1]). Such experiments and relevant theoretical studies are of particular value in this setting as they allow the study of quantum phenomena at the mesoscopic scale, but with an interesting additional twist: while the underlying quantum processes are purely linear, in the mean-field picture, interatomic interactions are accounted for

through an effective nonlinearity [see the last term in Eq. (1)] that significantly enriches the linear behavior.

An important modification of the linear behavior introduced by the above mentioned nonlinearity is that the underlying nonlinear GP model supports "fundamental" nonlinear structures in the form of matter-wave solitons and vortices. Importantly, such structures, and particularly dark [5], bright [6], and gap solitons [7], as well as vortices [8] and vortex lattices [9], have been observed in a series of experiments over the past decade. Moreover, experimental observation of dynamical features of these structures, such as the decay of dark solitons into vortex structures [10] has also been reported.

Here, we will focus on BECs with repulsive interatomic interactions, which support stable dark solitons and vortex structures, in quasi-one-dimensional (1D) and higher-dimensional settings, respectively. In that direction, and in connection with the above setting of interfering condensates, a very interesting observation was originally reported in Ref. [11]. In particular, it was numerically found that the collision of two quasi-1D BEC fragments upon release of the light sheet may lead to the formation of a train of dark solitons, filling the space originally covered by the light sheet. The phase of the condensate and its jumps around the soliton locations offered undisputed evidence that this nonlinear interference leads to the formation of the relevant localized nonlinear structures. Subsequent work in Ref. [12] aimed to clarify the regimes where the quasilinear interference of the original experiments [1] would result, versus the ones where the nonlinear interference of Ref. [11], forming dark soliton fringes, would arise. Importantly, new relevant experiments were very recently reported [13], in which three independent BECs interfered while trapped, giving rise to the formation of vortices. The latter experiment can rather naturally be characterized as a three-dimensional generalization of the original proposal of Ref. [11].

In the present work, we revisit the nonlinear interference problem of Ref. [11] in its higher-dimensional version, relevant to two-dimensional (2D) BECs (which are experimen-

---

*URL: http://nlds.sdsu.edu

023605-1

tally accessible [14]), as well to fully three-dimensional (3D) BECs. We use appropriately crafted potentials to slice the condensate in *two*, as well as in *four* parts in 2D settings and observe their nonlinear interference in these cases. Then, we fragment the 3D BEC into *two, four,* and *eight* pieces and examine the results of their merging as well. The main finding of the present work is that the nonlinear interference of higher-dimensional BECs typically gives rise to the higher-dimensional analogs of the 1D train of dark solitons. Specifically, in 2D, we find nucleation of vortex-antivortex pairs and vortex necklaces (which have previously been predicted to be formed in BECs as a result of the snaking instability of ring dark solitons [15]), while in 3D we find that the vortex patterns are replaced by vortex ring ones. The patterns created by the collision of different BEC slices become more complex for larger numbers of slices. In examining the robustness of the relevant mechanism, we also explore the role (in the vortex formation process) of the relative phases of the different fragments, as well as those of dissipation (emulating the interaction of the condensate with a noncondensed atom fraction) and of the time for ramping down the barrier separating the fragments.

Our presentation will be structured as follows. First, in Sec. II, we present the 2D version of the problem: the condensate is separated into two fragments by a light sheet and then allowed to collide (after the light sheet removal), producing vortex structures. In Sec. II, we also present results pertaining to the collision of four fragments separated by a light "cross." Next, in Sec. III, we systematically study the 3D case and interpret the corresponding findings for, respectively, two, four, and eight condensate fragments. Finally, in Sec. IV, we summarize and present our conclusions, as well as discuss some interesting aspects meriting future study.

II. TWO-DIMENSIONAL CONDENSATES

A. Collision of two in-phase fragments

In the 2D case, we propose two different experimentally feasible situations. In the more standard one, i.e., the direct analog of the 1D case of Ref. [11], the potential in Eq. (1) reads

$$V(x,y) = V_{HT}(x,y) + V_{LS}(x,y), \quad (2)$$

where, for the 2D case,

$$V_{HT}(x,y) = \frac{1}{2}\Omega^2(x^2 + y^2), \quad (3)$$

$$V_{LS}(x,y) = V_0 \,\text{sech}(by), \quad (4)$$

where V_{HT} represents the harmonic trapping potential (with Ω being the normalized trap strength), while V_{LS} is a localized repulsive potential describing the light sheet (with V_0 and b representing the normalized intensity and inverse width of the laser beam). Note that, similarly to the experiments of Ref. [13], the presence of V_{HT} is necessary to guarantee nonlinear interference of the two condensate fractions separated by the light sheet potential V_{LS} (the latter pushes the BEC atoms away from the vicinity of the line $y=0$).

In the case under consideration, the ground state of the system has the form shown in the top left panel in Fig. 1(a), namely, two identical condensate fragments separated by the light sheet. This ground state is obtained by relaxation (imaginary time integration) starting from a Thomas-Fermi cloud with density

$$|u_{TF}(x,y)|^2 = \max\{0, \mu - V(x,y)\}, \quad (5)$$

where μ is the chemical potential, which will be set to unity in what follows. Our proposed experiment assumes that the condensate, confined in the potential of Eq. (2) is in the ground state at $t=0$, and that both fragments share the *same* phase (see below for a description when fragments have different phases). Then, at that time, $t=0$, we "lift" (i.e., switch off) the light sheet by setting $V_0 \rightarrow 0$, and subsequently let the system evolve according to the GP Eq. (1). Notice that this is the direct generalization in 2D of the setup proposed in Ref. [11]. During the evolution, the two fragments originally constituting the condensate expand, and eventually interfere [see later times in the left column of Fig. 1(a)]. In order to quantify the amount of vorticity generated by the collision of the different fragments we monitor the vorticity $\omega(\mathbf{r},t)$ [$\mathbf{r}$ corresponds to (x,y) in the 2D simulations and (x,y,z) in the 3D simulations]. The vorticity is calculated as the curl of the fluid velocity $\mathbf{v}_s$, namely, $\omega(\mathbf{r},t)=\nabla \times \mathbf{v}_s$ (see, e.g., [16]), where the fluid velocity is given by

$$\mathbf{v}_s = \frac{u^* \nabla u - u \nabla u^*}{i|u|^2}. \quad (6)$$

The typical numerical experiment showing the collision between two fragments with the same initial phase ($\Delta\phi=0$, see below) shown in Fig. 1(a) is performed for $\Omega=0.1$, $V_0=5$, and $b=1$. This choice corresponds, e.g., to a pancake sodium BEC, containing $N \approx 300$ atoms, and confined in a trap with frequencies $\Omega_r=2\pi \times 10$ Hz and $\Omega_z=2\pi \times 100$ Hz. On the other hand, the light sheet parameters may correspond, e.g., to a blue-detuned laser beam providing a maximum barrier energy of $k_B \times 24$ nK. Note that the phenomenology that will be presented below does not change for the more realistic case of smaller trap strengths Ω, which leads to larger numbers of atoms.

Through the interference, quasi-1D "nonlinear" fringes are formed, i.e., dark stripes [see atom density at $t=8$ in the left panel of Fig. 1(a)] resembling dark solitons (in direct analogy to the 1D case), but now in the 2D setting. However, it is well known that such 1D stripes are unstable in 2D (and 3D) toward transverse modulations (see, e.g., Refs. [17–20] and references therein). As a result of the ensuing snaking instability, such stripes break up into vortex-antivortex pairs (because the original zero vorticity of the solution needs to be preserved). This is precisely what happens in our case as well. The bending of the stripes [see the atom density at $t=25$ in Fig. 1(a)] is responsible for the breakup into four vortex pairs as is shown in the vorticity plot at $t=25$. As the dark stripes continue bending and mixing, a series of vortex pair nucleations and annihilations occur.
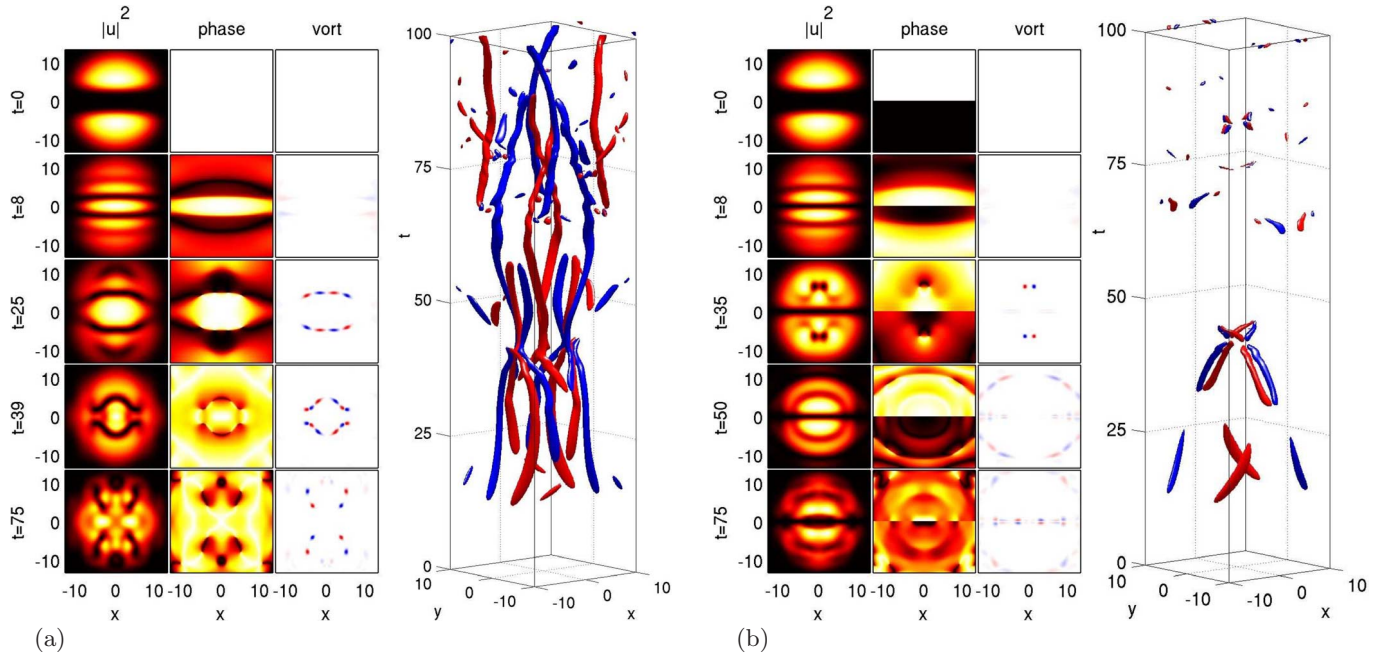
FIG. 1. (Color online) Collision of two condensate fragments originally separated by a quasi-one-dimensional light sheet lifted at $t=0$. Panels (a) correspond to fragments with the same initial phase ($\Delta\phi=0$) while panels (b) correspond to $\Delta\phi=\pi$. For each case, the first column of panels depicts the density of the condensate $|u(x,y,t)|^2$ at the times indicated (brighter regions indicate higher densities). The result of the release of the light sheet is the interference between the two fragments [see $|u(t=8)|^2$] that eventually leads to the nucleation of vortex pairs. The second column of panels depicts the corresponding phases (brighter regions indicate phases close to $-\pi$ and $+\pi$ while dark regions correspond to zero phase). The third column of panels depicts the corresponding fluid vorticity blue (red) indicates positive (negative) vorticity; see text. The fourth panel depicts the spatiotemporal evolution of the vorticity by showing a contour slice at a tenth of the maximum vorticity. The evolution is responsible for the nucleation and annihilation of vortex pairs resulting in the spatiotemporal vortex filaments shown in the panel. In all the 2D simulations, we use, for the spatial variable, a discretization of 301×301 sites centered around $(x,y)=(0,0)$. Also, the trap parameters for all 2D simulations are $\Omega=0.1$, $V_0=5$, and $b=1$.

To follow this evolution, we depict in the right panel of Fig. 1(a) a space-time plot of the vorticity. The main evolution of the vorticity can be summarized as follows. At $t\approx15$ four vortices (i.e., two vortex pairs) nucleate. Two more quartets of vortices are nucleated at $t\approx22$ and $t\approx35$. At $t\approx45$ the first quartet merges and is annihilated. The second quartet merges at $t\approx58$. This process of merging and spontaneous nucleation of vortex pairs and quartets remains active for long times (data not shown here).

B. The role of phase in two-fragment collisions

In actual BEC experiments (cf. Ref. [13]) the condensate is grown inside the *combined* harmonic trap V_{HT} and light sheet potential V_{LS}. There are two distinct regimes depending on the strength of the light sheet: if the latter potential is weak, the fragments have enough overlap and maintain a common phase; however, for stronger light sheets, the fragments grow essentially independently, carrying their own independent (random) phases. Another possibility in the experiment is to grow a condensate in the harmonic trap alone and then split the condensate into fragments by adiabatically ramping up the light sheet. Depending on the degree of adiabaticity and, more importantly, on the time the fragments are kept separate before releasing the light sheet, the phases of the different fragments will evolve independently and will,

effectively, randomize. Here, we explore the effects of such phase differences between the condensate fragments. We therefore consider the case where just before the light sheet release the phase of the top (bottom) fragment is ϕ_1 (ϕ_2). Without loss of generality we fix $\phi_1=0$ and we focus on the phase difference between the condensates $\Delta\phi\equiv\phi_2-\phi_1=\phi_2$. In Fig. 1(b) we depict the collision of two fragments as in Fig. 1(a) but with a different initial relative phase between the condensates of $\Delta\phi=\pi$. In the simulations, initial configurations with arbitrary phase differences $\Delta\phi$ were achieved by using the steady-state solution found for $\Delta\phi=0$ as before, then applying a phase shift of $\Delta\phi$ to the bottom fragment (i.e., for $y<0$), and running again the relaxation scheme (imaginary time integration) until convergence.

The results presented in Figs. 1(a) and 1(b) indicate that the detailed evolution of the vortex formation and merging depends on the relative phases of the condensates. In fact, further numerical results with phase differences between $\Delta\phi=0$ and π show similar vortex formation and annihilation with vortex "activity" decreasing (in terms of both the number of vortices produced and the persistence time of the structures) as $\Delta\phi$ was increased from 0 to π (results not shown here). It is interesting to note that the dynamics for phase differences different from zero loses its fourfold symmetry when compared to the $\Delta\phi=0$ case. In all cases that we tried, vortex pairs are nucleated at some point in the simulation irrespective of $\Delta\phi$. However, it is evident from the fig-
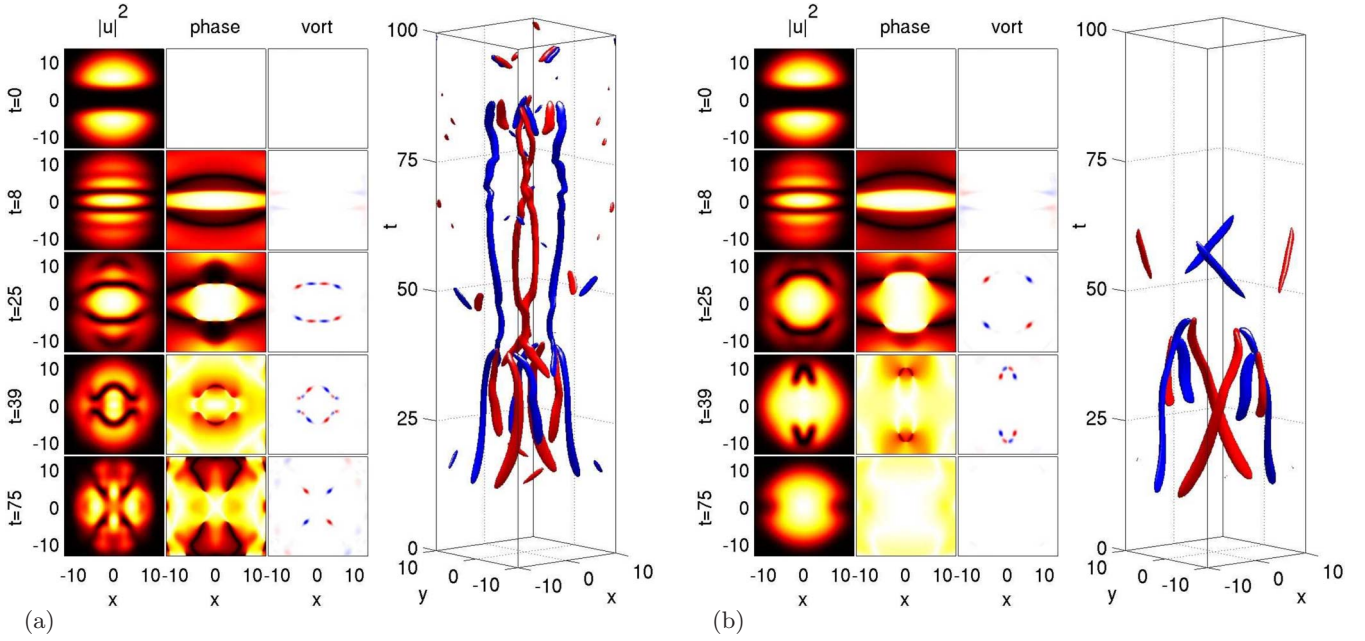
FIG. 2. (Color online) Effects of phenomenological damping on the collision of two condensate fragments with the same initial phase ($\Delta\phi=0$). The panels depict the same information as in Fig. 1(a) with the addition of phenomenological damping with $\gamma=0.005$ (a) and 0.1 (b).

ures that, the smaller the phase difference between the fragments, the more vortex structures are nucleated and the longer they live. In fact, the extreme case of a $\Delta\phi=\pi$ between fragments barely produces any vortex pairs [see Fig. 1(b)]. This is due to the fact that the initial condition is close to a steady-state domain wall (a dark soliton stripe separating out of phase domains) and thus there is little extra energy for the collision of the fragments. Indeed, as can be seen from Fig. 1(b) (where $\Delta\phi=\pi$), the condensate always maintains a configuration similar to a domain wall with some perturbations: the density always shows a nudge at $y=0$ and there is a predominant phase difference of π between the upper and lower half planes.

C. Dissipation and barrier ramping-down effects

The GP model used above relies, by construction, on the mean-field description of a boson gas at extremely low temperatures and becomes exact at $T=0$. When the temperature is finite, but still below the critical temperature T_c for BEC formation, there exists a fraction of atoms that is not condensed, the so-called thermal cloud. This thermal cloud is in fact coupled to the condensed gas and its presence produces effects that are not accounted for by the GP equation (cf. the insightful review in Chap. 18 of Ref. [21] and references therein). Phenomenologically, one of the most noticeable effects of the presence of a sizable thermal cloud is the introduction of damping (to the condensed gas). The approach of adding phenomenological damping to emulate thermal effects was originally proposed by Pitaevskii [22] and applied with a position-dependent loss rate in Ref. [23]. In practice, a few different implementations for the phenomenological damping are viable. Here, we follow the approach of Refs.

[24,25] where the GP equation is modified by the inclusion of a damping term, thus taking the form

$$(1-i\gamma)\frac{\partial}{\partial t}u = -\frac{1}{2}\nabla^2 u + V(\mathbf{r};t)u + |u|^2 u - \mu u, \qquad (7)$$

where γ is the damping rate (the chemical potential is again fixed at $\mu=1$). In Fig. 2 we display the collision of two fragments as in Fig. 1(a) (i.e., the same initial phase, $\Delta\phi=0$) for two values of damping. Figures 2(a) and 2(b) correspond to the cases of weak ($\gamma=0.005$) and strong ($\gamma=0.1$) damping. For the above choices, it is relevant to note that in Ref. [23] it was found that the value $\gamma=0.03$ corresponds to a temperature of about $0.1T_c$. As can be observed from the figure, the case of weak damping [$\gamma=0.005$, see Fig. 2(a)] behaves qualitatively the same as the case without damping [see Fig. 1(a)] until about $t=40$, when a noticeable reduction in the generated vorticity sets in. This effect is even more dramatic for larger damping [$\gamma=0.1$, see Fig. 2(b)] where it can be seen that after $t=65$ there is a complete absence of vortices. The effect of damping can be easily understood qualitatively in that the added phenomenological dissipation slows the fragments in their collisions and, therefore, less vorticity is produced.

We also studied the effect of ramp-down time of the laser sheet separating the different condensate fragments. In current experiments (see, e.g., Ref. [13]) the barrier created by the laser sheet can be removed using a gradual ramp-down of the laser intensity. Simulations (not shown here) reveal that slower ramping-down times have similar suppressing effects on vortex formation to the phenomenological damping cases described above. In fact, this is also for similar reasons, namely, that longer ramping-down times induce a slowing down of the fragments and hence the production of less vor-
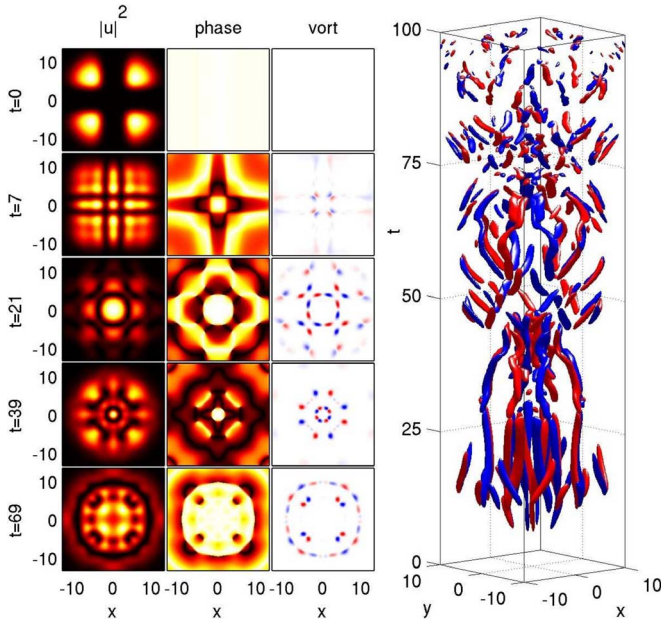
FIG. 3. (Color online) Similar to Fig. 1(a), but for an initial condition that contains four fragments [see $|u(t=0)|^2$], being the ground state of the potential of Eq. (8). Notice the fourfold symmetry of the interference in this case and the eventual formation of a complex pattern of vortex pairs. Same parameters as in Fig. 1 with $a=b=1$.

ticity. A more detailed study of the effects of ramp-down times on the vortex nucleation is beyond the scope of the present manuscript and will be reported in a separate presentation [26].

D. Collision of four in-phase fragments

The above cases represent 2D renderings of the setting as originally proposed in Ref. [11] (which, however, possesses a number of twists particular to 2D, as illustrated above). Nevertheless, a more genuinely 2D installment of the same "experiment" can also be envisioned and is proposed in Fig. 3. In this case, the light sheet potential is of the form

$$V_{LS} = V_0[\text{sech}(ax) + \text{sech}(by)], \qquad (8)$$

resulting in a ground state which contains four in-phase condensate fragments [as is shown by the initial density $|u(t=0)|^2$ in Fig. 3]. Subsequently, as the light cross is lifted at $t=0$, the fragments attempt to fill in the empty space, resulting in an interference pattern with fourfold symmetry. The oscillation and ensuing bending of the resulting dark stripes results in a rich evolution of vortex pairs as is shown by the space-time plot of the vorticity in the right panel of Fig. 3. Notice that, for this initial condition, more exotic patterns, including *vortex necklaces* (see also Ref. [15]) and structures with a higher number of vortices are formed. However, these patterns are considerably less long lived as compared to the ones observed in the numerical experiment with two in-phase fragments described above. A more detailed analysis of the role of different relative phases for the different fragments will be reported elsewhere [26].

III. THREE-DIMENSIONAL CONDENSATES

We now turn to the 3D analogs of the experiments proposed in the previous section. We start, once again, by a 3D version of the 1D suggestion of Ref. [11], with a harmonic trapping potential

$$V_{HT} = \frac{1}{2}\Omega^2(x^2 + y^2 + z^2), \qquad (9)$$

and a light sheet potential of the form

$$V_{LS} = V_0 \,\text{sech}(cz). \qquad (10)$$

We use $c=1$, in the typical results of Fig. 4, leading to the fragmentation of the initial condition into two pieces as is shown for $t=0$. Once the single light sheet of the potential of Eq. (10) is lifted, interference ensues among the different condensate fragments (see snapshots at $t=60,70,80$). As the two fragments get closer, pairs of *vortex rings* are nucleated between the fragments. It is interesting to observe that these vortex rings, created in pairs (recall that our system conserves angular momentum) around the condensate (like smoke rings that are created at the edge of a flow tube), may
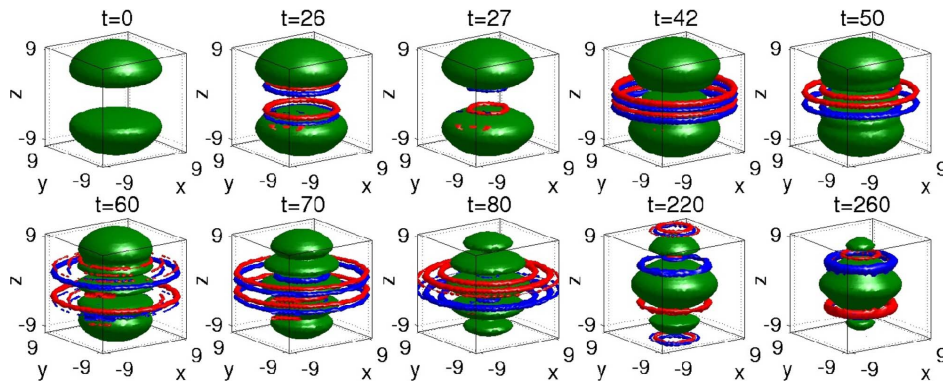

FIG. 4. (Color online) Collision of two 3D BEC fragments. A 3D contour plot of atomic density $|u(x,y,z,t)|^2$ at $\max(|u|^2)/2.5$ and the vorticity $\omega(x,y,z,t)$ at $\max(\omega)/15$ as a function of (x,y,z) at different times. Positively (negatively) charged vortex rings are depicted in blue (red). The spatial discretization is $50 \times 50 \times 50$ sites.
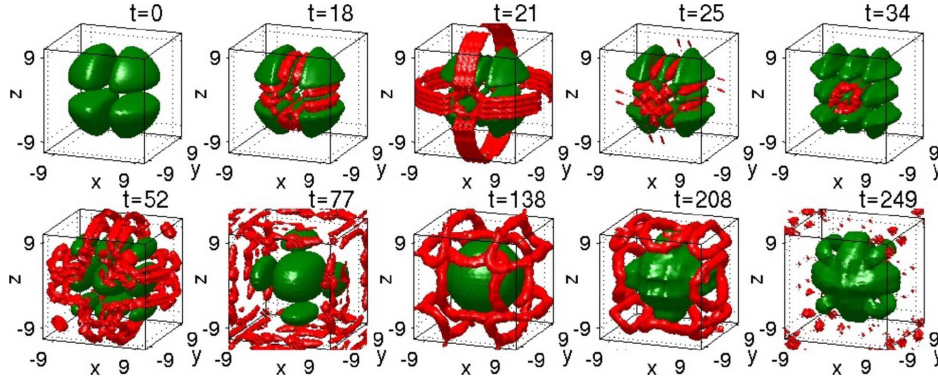
FIG. 5. (Color online) Similar to Fig. 4, but for an initial condensate with four fragments. In this case, both positively and negatively charged vortex rings, are depicted in red. Same parameters as in Fig. 4 with $a=c=1$.

travel inward and "pinch" the condensate, promoting its fragmentation. The formation of vortex rings in our system is reminiscent of the experimental realization of vortex rings induced by defects in Ref. [27]. Here, again, a complex process involving nucleation and annihilation of vortex rings persists for long times.

We now turn to the 3D analog of our second 2D numerical experiment, using a light cross potential

$$V_{\text{LS}} = V_0[\text{sech}(cz) + \text{sech}(ax)] \qquad (11)$$

to split the 3D condensate into four fragments initially, as shown at $t=0$ in Fig. 5. These four fragments start interfering, producing patterns with fringes possessing fourfold symmetry (see snapshots at $t=18,21,25,34$). A similar scenario, though more complex, as in the previous experiment takes place: in particular, we observe the formation of vortex rings around the condensate that promote the pinching of the different interference fragments. It is very interesting to note that for longer times ($t > 100$) a recurrent evolution emerges, whereby a cage of vortex rings surrounds the bulk of the condensate atoms (see the snapshots for $t=138$ and 208) alternating with turbulentlike patterns with vortices (see the

snapshots for $t=77$ and 249). This behavior seems to persist for long times (data not shown here).

Finally, in the same spirit as followed above, one can attempt to produce a genuinely 3D version of this setup, by splitting the condensate into eight fragments as is shown in Fig. 6. This can be done through a 3D light sheet (consisting of three mutually perpendicular 1D light sheets):

$$V_{\text{LS}} = V_0[\text{sech}(ax) + \text{sech}(by) + \text{sech}(cz)]. \qquad (12)$$

As a result of releasing the light sheets, the fragments interfere with an eightfold symmetry (see snapshots at $t=36,40$ in Fig. 6). Again we find that vortex rings are created in pairs around the condensate and subsequently migrate inward, promoting the pinching of the interference pattern. We also find the same recurrence phenomenon as in the previous experiment with four fragments, whereby a cage of vortex rings surrounds the bulk of the condensate (see the snapshots at $t=139,191,209$) alternating with vortex-rich, turbulentlike states (see the snapshot at $t=247$). Yet again this alternating behavior seems to persist for longer times (data not shown here). A general observation for the experiments with the two and three light sheets (in comparison with the more straightforward realization with one such sheet) is that vortex rings
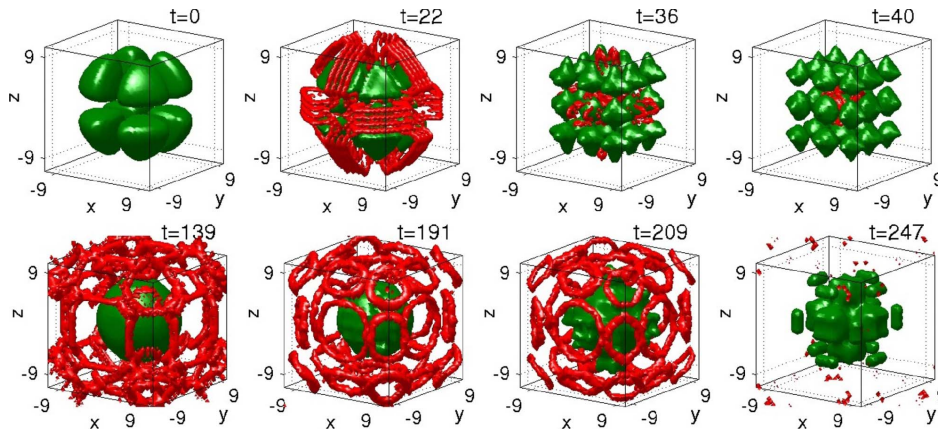

FIG. 6. (Color online) This last 3D case is similar to the earlier ones, but for an initial condensate with eight fragments. In this case also, both positively and negatively charged vortex rings are depicted in red. Same parameters as in Fig. 4 with $a=b=c=1$.

have a shorter lifetime and are harder to detect due to the complicated nature of the dynamics. This observation is, in principle, also true for the 2D case (as can be seen by comparing the two-light-sheet case with that of a single light sheet). Hence, perhaps the most robust and straightforward configuration for observing the nonlinear interference dynamics and the formation of vortices and vortex rings, respectively, in 2D and 3D consists of the quasi-1D configuration with two fragments (and a single light sheet) in each case.

IV. CONCLUSIONS AND CHALLENGES

In the present work, we have discussed a series of numerical experiments, representing generalizations of the original suggestion of Ref. [11] for a nonlinear interference, leading to the formation of fundamental nonlinear structures. Importantly, relevant experiments with higher-dimensional BECs (in a slightly different configuration than the one proposed here) demonstrating this concept have been reported very recently [13].

While in the 1D example of Ref. [11], the ensuing nonlinear waves were robust dark solitons, in 2D and 3D settings the situation is considerably more complex, even though fundamental nonlinear structures still emerge. In the 2D setting, corresponding to a pancake condensate, we find that slicing the condensate with a light sheet or a light cross gives rise to interference patterns and the nucleation of vortex pairs. This is the situation most reminiscent of the experiment of Ref. [13] (although the latter involved the merger of three fragments), where vortex creation was observed as well. In our case, subsequently, a complex cascade of vortex pair annihilations and nucleations was found to persist for long times. Some vortex "necklaces" were also seen to be stable for long times. This is particularly the case for a BEC fragmented into two pieces, whereas the vortex patterns in the four fragments case have shorter lifetimes, and thus it is expected that it would be more difficult to observe them experimentally.

In the simpler case of two fragments in 2D, we studied the effects of different phases between the condensate fragments. An interesting extension of the results presented herein is the study of the role of the phase difference between fragments in a condensate with more than two fragments [26]. We also analyzed the suppressing effects of phenomenological damping (induced by coupling with the thermal cloud) and briefly discussed the similar role of the ramping-down of the light sheet on the formation of vorticity.

The 3D setting is particularly interesting, since the 2D vortex patterns are replaced by vortex ring ones. We find that these vortex rings, upon nucleating in pairs around the condensate, migrate inward, promoting the pinching of the different interference patterns. Subsequently the condensate evolves under a complex pattern of nucleation and annihilation of vortex rings. More interesting, however, is the observation that for longer times the condensate seems to alternate between a pattern consisting of a vortex ring cage around the bulk of the condensed atoms and a pattern of turbulentlike vorticity.

An immediately interesting ramification of our study would be to compare and contrast the situation where the condensate fragments originate from one component with that where they may originate from different components [28]. Such interference experiments, in part, already exist [29] and have interesting consequences regarding the character of the interaction of the two components. It would be interesting to examine whether such interactions can lead to (possibly anticorrelated) vortices and vortex rings in the two-component condensate. Such studies are currently in progress and will be reported elsewhere.

[1] M. R. Andrews, C. G. Townsend, H.-J. Miesner, D. S. Durfee, D. M. Kurn, and W. Ketterle, Science **275**, 637 (1997).

[2] A. Röhrl, M. Naraschewski, A. Schenzle, and H. Wallis, Phys. Rev. Lett. **78**, 4143 (1997).

[3] L. P. Pitaevskii and S. Stringari, *Bose-Einstein Condensation* (Oxford University Press, Oxford, 2003); C. J. Pethick and H. Smith, *Bose-Einstein Condensation in Dilute Gases* (Cambridge University Press, Cambridge, U.K., 2002).

[4] P. G. Kevrekidis, R. Carretero-González, D. J. Frantzeskakis, and I. G. Kevrekidis, Mod. Phys. Lett. B **18**, 1481 (2004).

[5] S. Burger, K. Bongs, S. Dettmer, W. Ertmer, K. Sengstock, A. Sanpera, G. V. Shlyapnikov, and M. Lewenstein, Phys. Rev. Lett. **83**, 5198 (1999); J. Denschlag, J. E. Simsarian, D. L. Feder, C. W. Clark, L. A. Collins, J. Cubizolles, L. Deng, E. W. Hagley, K. Helmerson, W. P. Reinhardt, S. L. Rolston, B. I. Schneider, and W. D. Phillips, Science **287**, 97 (2000).

[6] K. E. Strecker, G. B. Partridge, A. G. Truscott, and R. G. Hulet, Nature (London) **417**, 150 (2002); L. Khaykovich, F. Schreck, G. Ferrari, T. Bourdel, J. Cubizolles, L. D. Carr, Y. Castin, and C. Salomon, Science **296**, 1290 (2002).

[7] B. Eiermann, Th. Anker, M. Albiez, M. Taglieber, P. Treutlein, K.-P. Marzlin, and M. K. Oberthaler, Phys. Rev. Lett. **92**, 230401 (2004).

[8] M. R. Matthews, B. P. Anderson, P. C. Haljan, D. S. Hall, C. E. Wieman, and E. A. Cornell, Phys. Rev. Lett. **83**, 2498 (1999); S. Inouye, S. Gupta, T. Rosenband, A. P. Chikkatur, A. Görlitz, T. L. Gustavson, A. E. Leanhardt, D. E. Pritchard, and W. Ketterle, *ibid.* **87**, 080402 (2001).

[9] K. W. Madison, F. Chevy, W. Wohlleben, and J. Dalibard, Phys. Rev. Lett. **84**, 806 (2000); J. R. Abo-Shaeer, C. Raman, J. M. Vogels, and W. Ketterle, Science **292**, 476 (2001); J. R. Abo-Shaeer, C. Raman, and W. Ketterle, Phys. Rev. Lett. **88**, 070409 (2002); P. Engels, I. Coddington, P. C. Haljan, and E. A. Cornell, *ibid.* **89**, 100403 (2002).

[10] B. P. Anderson, P. C. Haljan, C. A. Regal, D. L. Feder, L. A. Collins, C. W. Clark, and E. A. Cornell, Phys. Rev. Lett. **86**, 2926 (2001); Z. Dutton, M. Budde, C. Slowe, and L. V. Hau, Science **293**, 663 (2001).

[11] W.P. Reinhardt and C.W. Clark, J. Phys. B **30**, L785 (1997).

[12] T. F. Scott, R. J. Ballagh, and K. Burnett, J. Phys. B **31**, L329 (1998).

[13] D. R. Scherer, C. N. Weiler, T. W. Neely, and B. P. Anderson, Phys. Rev. Lett. **98**, 110402 (2007).

[14] A. Görlitz, J. M. Vogels, A. E. Leanhardt, C. Raman, T. L. Gustavson, J. R. Abo-Shaeer, A. P. Chikkatur, S. Gupta, S. Inouye, T. Rosenband, and W. Ketterle, Phys. Rev. Lett. **87**, 130402 (2001).

[15] G. Theocharis, D. J. Frantzeskakis, P. G. Kevrekidis, B. A. Malomed, and Yu. S. Kivshar, Phys. Rev. Lett. **90**, 120403 (2003).

[16] B. Jackson, J. F. McCann, and C. S. Adams, Phys. Rev. Lett. **80**, 3903 (1998).

[17] Yu. S. Kivshar and B. Luther-Davies, Phys. Rep. **298**, 81 (1998).

[18] A. E. Muryshev, H. B. van Linden van den Heuvell, and G. V. Shlyapnikov, Phys. Rev. A **60**, R2665 (1999); D. L. Feder, M. S. Pindzola, L. A. Collins, B. I. Schneider, and C. W. Clark, *ibid.* **62**, 053606 (2000).

[19] P. G. Kevrekidis, G. Theocharis, D. J. Frantzeskakis, and A. Trombettoni, Phys. Rev. A **70**, 023602 (2004).

[20] P. G. Kevrekidis and D. J. Frantzeskakis, Mod. Phys. Lett. B **18**, 173 (2004).

[21] *Emergent Nonlinear Phenomena in Bose-Einstein Condensates: Theory and Experiment*, edited by P. G. Kevrekidis, D. J. Frantzeskakis, and R. Carretero-González, Springer Series on Atomic, Optical, and Plasma Physics Vol. 45 (Springer, Berlin, 2008).

[22] L. P. Pitaevskii, Sov. Phys. JETP **35**, 282 (1959).

[23] S. Choi, S. A. Morgan, and K. Burnett, Phys. Rev. A **57**, 4057 (1998).

[24] M. Tsubota, K. Kasamatsu, and M. Ueda, Phys. Rev. A **65**, 023603 (2002).

[25] K. Kasamatsu, M. Tsubota, and M. Ueda, Phys. Rev. A **67**, 033610 (2003).

[26] R. Carretero-González, B. P. Anderson, P. G. Kevrekidis, D. J. Frantzeskakis, and C. N. Weiler, Phys. Rev. A (in press, 2008).

[27] N. S. Ginsberg, J. Brand, and L. V. Hau, Phys. Rev. Lett. **94**, 040403 (2005).

[28] M.-O. Mewes, M. R. Andrews, D. M. Kurn, D. S. Durfee, C. G. Townsend, and W. Ketterle, Phys. Rev. Lett. **78**, 582 (1997); C. J. Myatt, E. A. Burt, R. W. Ghrist, E. A. Cornell, and C. E. Wieman, *ibid.* **78**, 586 (1997).

[29] M. H. Wheeler, K. M. Mertes, J. D. Erwin, and D. S. Hall, Phys. Rev. Lett. **93**, 170402 (2004).